Applied Physics Letters

Dual-color ultraviolet photodetector based on mixed-phase-MgZnO/i-MgO/p-Si double heterojunction

X. H. Xie, Z. Z. Zhang, C. X. Shan, H. Y. Chen, and D. Z. Shen

Citation: Appl. Phys. Lett. **101**, 081104 (2012); doi: 10.1063/1.4746772

View online: http://dx.doi.org/10.1063/1.4746772

View Table of Contents: http://apl.aip.org/resource/1/APPLAB/v101/i8

Published by the American Institute of Physics.

Dual-color ultraviolet photodetector based on mixed-phase-MgZnO/i-MgO/p-Si double heterojunction

X. H. Xie,[1,2] Z. Z. Zhang,[1,a)] C. X. Shan,[1] H. Y. Chen,[1,2] and D. Z. Shen[1,a)]
[1]*State Key Laboratory of Luminescence and Applications, Changchun Institute of Optics, Fine Mechanics and Physics, Chinese Academy of Sciences, Changchun 130033, People's Republic of China*
[2]*Graduate University of the Chinese Academy of Sciences, Beijing 100049, People's Republic of China*

(Received 18 June 2012; accepted 3 August 2012; published online 20 August 2012)

We report a dual-color ultraviolet (UV) photodetector based on mixed-phase-MgZnO/i-MgO/p-Si double heterojunction. The device exhibits distinct dominant responses at solar blind (250 nm) and visible blind (around 330 nm) UV regions under different reverse biases. By using the energy band diagram of the structure, it is found that the bias-tunable two-color detection is originated from different valence band offset between cubic MgZnO/MgO and hexagonal MgZnO/MgO. Meanwhile, due to the large conduction band offset at the Si/MgO interface, the visible-light photoresponse from Si substrate is suppressed. © *2012 American Institute of Physics*.
[http://dx.doi.org/10.1063/1.4746772]

Wide bandgap $Mg_xZn_{1-x}O$ alloy has received increasing intense attention due to its large tunable bandgap, from 3.37 eV of wurtzite (WZ) ZnO to 7.8 eV of rock salt (RS) MgO,[1] which makes it a promising candidate for deep ultraviolet (DUV) optoelectronic devices, in principle. Until now, various kinds of MgZnO-based light generation and detection devices have been demonstrated.[2,3] Especially, in the field of ultraviolet (UV) detection, some important progress has been achieved.[4–6] However, phase segregation of MgZnO often occurs, because of the different crystal structure between WZ-ZnO and RS-MgO, either in the growth process or post-annealing, when the Mg content is in the range of 37% to 62%.[7,8] Several approaches have been taken toward realizing a single-phase MgZnO with a designated bandgap, whether RS or WZ.[6,9] Nevertheless, phase segregation is still an obstacle for practical applications. The mixed-phased (MP) MgZnO has two band gaps,[8] corresponding to the solar blind (220 to 280 nm) and visible blind (300 to 360 nm), respectively. Based on this, from the opposite point of view, it is also a unique advantage, which is not found in other wide-bandgap semiconductor materials (such as AlGaN, SiC, diamond, etc.). In other words, MP-MgZnO makes detecting double wavelength, solar blind and visible blind, in a single detector by one type materials system more easy. It is known that Si microelectronic technology was well developed. Furthermore, taking into account the energy band offsets, MgZnO/Si heterojunctions will become more practical and competitive in dual-wavelength, detecting by monolithically and vertically integrated configuration. So far, some researches related to MgZnO/Si heterojunction have been taken.[10,11] However, dual-wavelength detector, utilizing MP-MgZnO/Si, has not been reported.

In this work, by constructing p-i-n typed double heterojunction (DH) based on (MP-MgZnO film)/(insulator MgO)/(p-type Si film), we demonstrated a dual-color (solar blind and visible blind) UV photodetector with dual response peaks at 250 and 325 nm at zero-bias, corresponding to the bandgap values of WZ- and RS-MgZnO. The responsivity ratio of the two peaks depends sensitively on the bias. Moreover, the visible-light photoresponse from Si substrate was suppressed in the detector. To illuminate the experimental results, an energy band diagram of MP-MgZnO/i-MgO/p-Si was proposed according to Anderson model.

The MP-MgZnO film of about 500 nm was grown on a p-type Si (111) substrate with a MgO sandwich layer about 60 nm by metal-organic chemical vapor deposition (MOCVD). Polished p-type silicon substrates were cleaned by RCA method. Oxygen (O_2), diethylzinc (DEZn), and dimethyl dicyclopentadienyl magnesium ($MeCp_2Mg$) were employed as the precursors. Nitrogen with 5N-purity was used as the carrier gas. Both the layers of the heterostructure were grown at 450 °C, keeping the chamber pressure at 150 Torr. To ensure a narrow depletion region at MP-MgZnO side to separate the photo-generated carriers effectively, gallium (Ga) was incorporated into the MP-MgZnO film as the n-type dopant by using triethylgallium (TEGa) as dopant. A reference Ga-doped MP-MgZnO film grown on a c-plane sapphire substrate with the same growth conditions was used to examine Ohmic contact of metal electrodes on the film. A circular indium film (~400 nm) and a gold film (~50 nm) were deposited on the backside of the p-Si substrate and MP-MgZnO as the electrodes, respectively, by thermal evaporation method. Hall measurement system (Lakeshore HMS7707) was utilized for current-voltage (I-V) characterization of the DH structure. The structural characterization of the film was evaluated by an x-ray diffraction (XRD) with Cu-Kα 0.154 nm line as the radiation source. The spectral response of the dual-color p-i-n photodetector was measured using a 150 W Xe lamp, a monochromator, an optical chopper (EG&G 192), and a lock-in amplifier (EG&G 124A) in a synchronous detection scheme. The morphology of the MP-MgZnO film (top view) was examined with a scanning electron microscope (SEM) (HITACHI S-4800).

The MP-MgZnO/i-MgO/p-Si epitaxial heterostructure was used to construct a dual-color photodetector device as illustrated in the inset of Fig. 1. As shown in Figure 1, the p-i-n junction shows clear rectifying characteristics with a

a)Authors to whom correspondence should be addressed. Electronic addresses: exciton@163.com and dzshen824@sohu.com.

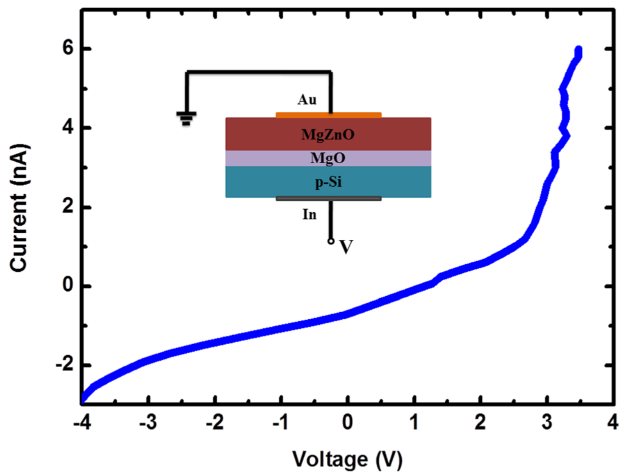

FIG. 1. Current-voltage (I-V) characteristic curve of the Au/MP-MgZnO/i-MgO/p-Si/In double heterojunction photodetector. The inset shows the schematic configuration of the double heterojunction photodetector structure.

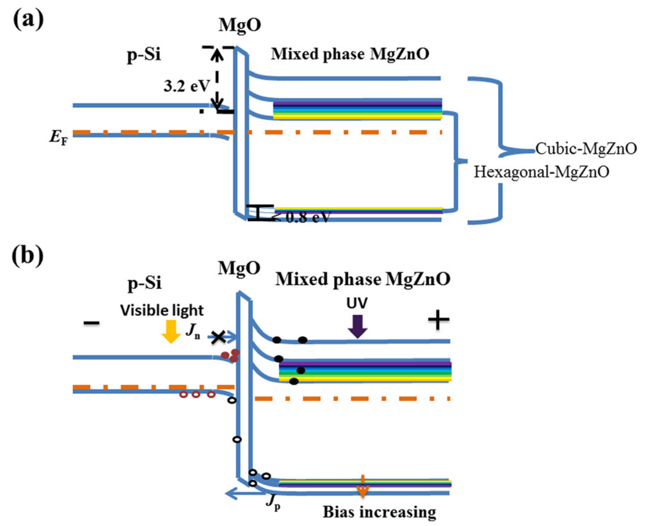

FIG. 3. Schematic diagram showing the band alignment of the MP-MgZnO/MgO/p-Si double heterojunction: (a) under equilibrium condition and (b) under illumination at different reverse bias.

threshold voltage of about 2.0 V. The Ohmic contact of the Au electrode on the MP-MgZnO layer and In/p-Si is confirmed by the linear I-V curve (not shown here).

The top-view SEM images of the MP-MgZnO films grown on the p-Si (111) substrate are shown in the inset of Fig. 2(a). Both triangular and hexagonal grains were observed, corresponding to RS-(111) and WZ-(002) crystalline orientation characters, respectively. The XRD patterns also indicated the mixed-phased structure of the MgZnO films, as shown in Fig. 2(a), which provide a material basis for dual-color detection. Fig. 2(b) depicts the normalized spectral response of the device measured in normal incidence geometry at different applied biases. As seen, both responses at UVC and UVA ranges, which corresponding to solar blind and visible blind bands, are observed. At zero-bias, the response to UVC is dominant. With increasing reverse applied voltages, UVA response dominates the spectra gradually. Meanwhile, the response peak shifts from 325 to 350 nm (see below for further discussion). There are no changes in FWHM of the two responses. The peak response of UVA increases with the reverse bias arising, meanwhile the peak response of UVC just has a little change, as illustrated in the Fig. 2(c). The two distinct response peaks at 250 nm and around 330 nm have demonstrated the capability of the device for dual-color detections under different biases.

To explain the operation mechanisms of the dual-color photodetector, band diagrams derived from Anderson model are shown in Fig. 3. According to the electron affinity (χ) of 4.05,[12] 0.8 eV (Ref. 13) and band gap of 1.12, 7.8 eV (Ref. 1) for Si and MgO, respectively, the conduction band offset (CBO) at the Si/MgO interface is calculated to be 3.2 eV.

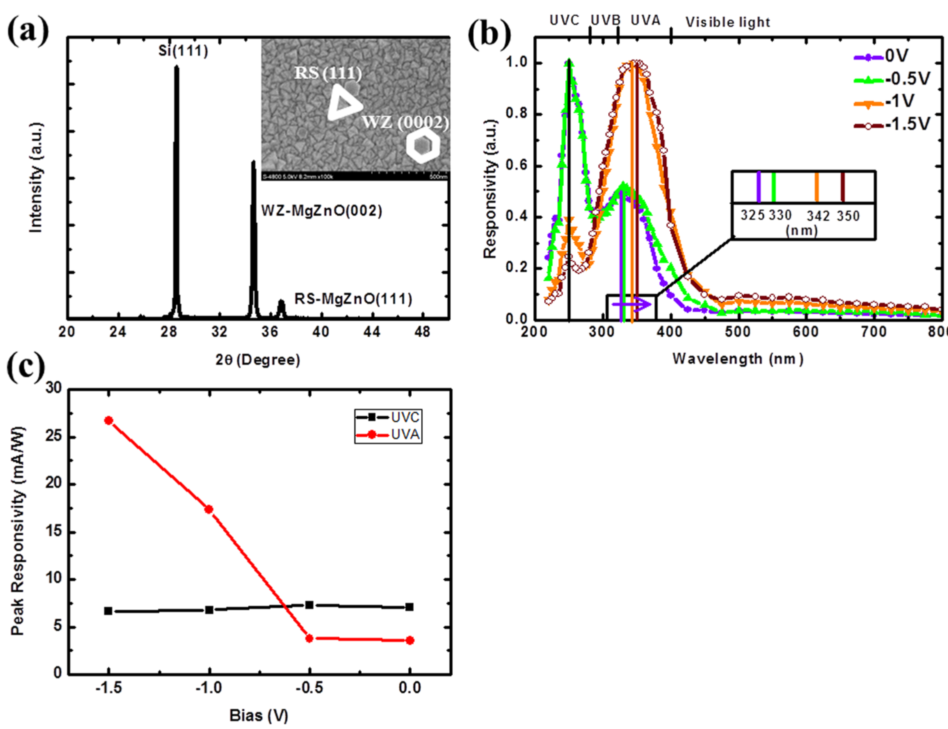

FIG. 2. (a) θ-2θ XRD spectrum of the MP-MgZnO films, the inset shows the scanning electron microscopy (SEM) images of MP-MgZnO grown on the p-Si substrate. (b) Photoresponse spectra of the DH photodetector at different bias voltages measured in the normal incidence geometry. (c) The peak response of UVA and UVC individually as a function of bias.

Meanwhile, from the χ (4.35 eV (Ref. 14)) and band gap (3.37 eV) for ZnO, the electron affinity of $Mg_xZn_{1-x}O$ can be estimated by linear fitting from those of ZnO and MgO. Therefore, an energy barrier for holes no larger than 0.8 eV will appear at the MgO/MP-MgZnO interface. Under thermal equilibrium, as a result of carrier diffusion, the depletion regions will be formed in both Si and MP-MgZnO sides, and then the Femi level became constant across the entire region of the DH. Taking into account the more non-uniform composition,[15,16] the band gap of WZ-MgZnO will possess a larger fluctuation than that of RS-phase. It answers the red shift of photoresponse peak in the UVA range (discussed below) [Fig. 3(a)]. As illustrated in the schematic in Fig. 3(b), when the detector is under UV and visible illumination, the photogenerated carriers were driven by built-in electric field. However, the visible-light generated electrons from p-Si side cannot cross over the (p-Si)/(i-MgO) interface due to the high barrier (3.2 eV), and then recombine with holes immediately. So, the visible-light photoresponse from Si substrate was suppressed. On the other side, photogenerated holes in the MP-MgZnO layer will transmit through i-MgO layer because of the relatively low barrier (no larger than 0.80 eV) at the MP-MgZnO/i-MgO interface. It endows the device with a UV photoresponse function. Furthermore, at a zero-bias or a small reverse bias, since the valence band maximum (VBM) of RS-MgZnO is much lower than the WZ phase (about 400 meV),[17,18] the UVC photogenerated holes from RS phase can cross the MgO layer in larger quantities than that from WZ parts. With increasing the reverse bias, the Fermi level in MP-MgZnO moves downward, so that UVA photo-holes from the WZ parts can cross the barrier at (i-MgO)/(p-Si) interface by Fowler-Nordheim tunneling or trap-assisted tunneling. Therefore, the UVA peak dominates the response and red shifts gradually as the reverse bias is increased to a certain degree.

In conclusion, a dual-color UV photodetector based on MP-MgZnO/i-MgO/p-Si DH structure was fabricated and characterized. Two photoresponse peaks, located at UVC (250 nm) and UVA (around 330 nm) range, were observed at different reverse bias. It was attributed to the change of the interface barrier under the increasing reverse bias. It indicates that MP-MgZnO is a promising candidate for UV dual- or even multi-wavelength detector.

This work was supported by the National Basic Research Program of China (973 Program) under Grant Nos. 2011CB302002 and 2011CB302006, the National Natural Science Foundation of China under Grant Nos. 11134009 and 10974197.

[1]M. W. Williams and E. T. Arakawa, J. Appl. Phys. **38**, 5272 (1967).
[2]H. Zhu, C. X. Shan, B. H. Li, Z. Z. Zhang, B. Yao, and D. Z. Shen, Appl. Phys. Lett. **99**, 101110 (2011).
[3]Z. G. Ju, C. X. Shan, D. Y. Jiang, J. Y. Zhang, B. Yao, D. X. Zhao, D. Z.Shen, and X. W. Fan, Appl. Phys. Lett. **93**, 173505 (2008).
[4]H. L. Liang, Z. X. Mei, Q. H. Zhang, L. Gu, S. Liang, Y. N. Hou, D. Q. Ye, C. Z. Gu, R. C. Yu, and X. L. Du, Appl. Phys. Lett. **98**, 221902 (2011).
[5]Z. Zhang, H. von Wenckstern, M. Schmidt, and M. Grundmann, Appl. Phys. Lett. **99**, 083502 (2011).
[6]L. K. Wang, Z. G. Ju, J. Y. Zhang, J. Zheng, D. Z. Shen, B. Yao, D. X. Zhao, Z. Z. Zhang, B. H. Li, and C. X. Shan, Appl. Phys. Lett. **95**, 131113 (2009).
[7]M. Wei, R. C. Boutwell, J. W. Mares, A. Scheurer, and W. V. Schoenfeld, Appl. Phys. Lett. **98**, 261913 (2011).
[8]Z. G. Ju, C. X. Shan, C. L. Yang, J. Y. Zhang, B. Yao, D. X. Zhao, D. Z. Shen, and X. W. Fan, Appl. Phys. Lett. **94**, 101902 (2009).
[9]X. L. Du, Z. X. Mei, Z. L. Liu, Y. Guo, T. C. Zhang, Y. N. Hou, Z. Zhang, Q. K. Xue, and A. Yu. Kuznetsov, Adv. Mater. (Weinheim, Ger.) **21**, 4625 (2009).
[10]P. Chen, X. Ma, D. Li, Y. Zhang, and D. Yang, J. Appl. Phys. **102**, 083106 (2007).
[11]W. Yang, S. S. Hullavarad, B. Nagaraj, I. Takeuchi, R. P. Sharma, T. Venkatesan, R. D. Vispute, and H. Shen, Appl. Phys. Lett. **82**, 3424 (2003).
[12]D. G. Baik and S. M. Cho, Thin Solid Films **354**, 227 (1999).
[13]J. Yamashita, Phys. Rev. **111**, 733 (1958).
[14]Julio A. Aranovich, D. Golmayo, A. L. Fahrenbruch, and R. H. Bube, J. Appl. Phys. **51**, 4260 (1980).
[15]Z. L. Liu, Z. X. Mei, R. Wang, J. M. Zhao, H. L. Liang, Y. Guo, A. Yu. Kuznetsov, and X. L. Du, J. Phys. D: Appl. Phys. **43**, 285402 (2010).
[16]I. V. Maznichenko, A. Ernst, M. Bouhassoune, J. Henk, M. Däne, M. Lüders, P. Bruno, W. Hergert, I. Mertig, Z. Szotek, and W. M. Temmerman, Phys. Rev. B **80**, 144101 (2009).
[17]A. Ohtomo, M. Kawasaki, I. Ohkubo, H. Koinuma, T. Yasuda, and Y. Segawa, Appl. Phys. Lett. **75**, 980 (1999).
[18]Y. F. Li, B. Yao, Y. M. Lu, B. H. Li, Y. Q. Gai, C. X. Cong, Z. Z. Zhang, D. X. Zhao, J. Y. Zhang, D. Z. Shen, and X. W. Fan, Appl. Phys. Lett. **92**, 192116 (2008).